Optical Characteristics of Aerosol Trioxide Dialuminum at the IR Wavelength Range

O.K. Voitsekhovskaya[1], O.V. Shefer*[2], D.E. Kashirskii[3]

[1]Department of Quantum Electronics & Photonics, Radiophysics faculty, National Research Tomsk State University, Tomsk, Russia
[2] Institute of Cybernetics, National Research Tomsk Polytechnic University, Tomsk, Russia
[3]Academician V.D. Kuznetsov's Siberian Physical-Technical R&D Institute, National Research Tomsk State University, Tomsk, Russia

ABSTRACT

In this work, a numerical study of the transmission function, extinction coefficient, scattering coefficient, and absorption coefficient of the aerosol generated by the jet engine emissions was performed. Analyzing the calculation results of the IR optical characteristics of anthropogenic emissions containing the dialuminum trioxide was carried out. The spectral features of the optical characteristics of the medium caused by the average size, concentration and complex refractive index of the particles were illustrated.

Aerosol, dialuminum trioxide, optical characteristics, IR radiation

1. INTRODUCTION

The rocket and aircraft engines are the principal anthropogenic emission sources into the upper and middle atmosphere. The engine quality could affect the in-flight safety and the ecological state of the atmosphere.

As a rule, the engine protection system uses the sensors mounted into the engine to monitor its status. This complicates the engine tests. The optical methods provide remote monitoring of the aircraft engine state [1]. These methods do not require any modifications of engines, and this is a major advantage of this technique. Due to low inertia, optical methods allow to obtain information in real time and if necessary to give a warning. The optical monitoring method reveals the engine parts corrosion by using the spectral lines of metals. Other methods can not reveal these failures. The optical methods of the engine monitoring analyze the absorption or emission spectra of the engine exhaust. These methods provide information on the concentration of particles of the constructional materials and estimate the engine cycle life in real time. This helps the engineers prevent the accidents. New types of the solid propellants contain the ultradisperse aluminum powder and an ammonium perchlorate oxidizer [2] that requires an analysis of the solid rocket motor exhaust. The effective optical monitoring requires a reliable data on the absorption spectra of metallic aerosols, such as the dialuminum trioxide (Al_2O_3).

2. METHOD OF CALCULATION

For numerical simulations of effects caused by the transformation of the radiation beam passing through a polydisperse medium, it is necessary to consider a model for a single particle. This model allows to determine a dependence of the light scattering characteristics on parameters of the incident radiation and the particle properties. To calculate the optical properties of the aerosol, the Mie theory [2] was used. The Mie solution for the plane wave scattering by a sphere is a multipurpose approach used in the light scattering theory. This approach can be used to model a medium that contains both small and large particles of various forms (both spherical and nonspherical particles).

* shefer-ol@mail.ru

21st International Symposium on Atmospheric and Ocean Optics: Atmospheric Physics, edited by G. G. Matvienko, O. A. Romanovskii, Proc. of SPIE Vol. 9680, 96803A

When modeling the radiation extinction by a disperse medium, it is necessary to consider the extinction coefficient. The extinction coefficient of an ensemble of particles is expressed in terms of the extinction cross section of an individual particle in the following way:

$$\alpha_{ext} = C \cdot \langle S_{ext} \rangle . \quad (1)$$

Here $\langle S_{ext} \rangle$ is average extinction cross section, and C is the concentration of particles in the volume element. To test a model for calculating the extinction coefficient, resulted from the energy conservation law (extinction = scattering + absorption) expression was used:

$$\alpha_{ext} = \alpha_{abs} + \alpha_{sca} , \quad (2)$$

where α_{ext} is the extinction coefficient, α_{abs} is the absorption coefficient, and α_{sca} is the scattering coefficient.
When radiation energy flux passes through a disperse medium, this results in the light scattering by particles in all directions and conversion of the absorbed energy to heat energy. The attenuation of the radiation beam transmitted through a layer of the polydisperse medium is described by the expression:

$$I_{trans} = I_i \cdot T , \quad (3)$$

where I_{trans} is the intensity of the transmitted radiation, I_i is the intensity of the incident radiation, and T is the transmission function (TF).
The transmission function of the aerosol medium with thickness *h* is defined as

$$T = \exp(-\alpha_{ext} \cdot h). \quad (4)$$

Optical properties of the polydisperse medium including the dialuminum trioxide particles are studied in this work. We considered various average sizes and concentrations of particles in the volume element.

3. RESULTS AND DISCUSSION

The transmission function, scattering coefficient, absorption coefficient, and extinction coefficient in IR range for a radiation beam passing through an ensemble of spherical particles were investigated numerically. The calculations were based on the following input parameters: the particle sizes (the radius R), the complex refractive index ($\tilde{n} = n + i \cdot \chi$, where *n* describes the refraction, and χ is the absorption coefficient), the volume concentration of particles (C), and wavelength of the incident radiation (λ).

We specified the microphysical and optical properties of the disperse medium using the following *a priori* data: the particle sizes vary from 0.01 μm to 20 μm; the particle concentration varies from 10^5 to 10^7 l^{-1} [3]; the optical properties of the Al_2O_3 were taken from [4].

Fig. 1 shows the wavelength dependence of the refraction index $n=n(\lambda)$ and the absorption index $\chi=\chi(\lambda)$ according to data from the paper [4]. The refraction index $n=n(\lambda)$ has the minimum value ($n\approx0.66$) at $\lambda\approx10.97$ μm. This resulted from a resonant interaction of optical radiation with the Al_2O_3 lattice. In the near-infrared range $n >> \chi$. If the radiation wavelength $\lambda<10$ μm, the radiation attenuation is determined mostly by the light scattering. The real and imaginary parts of the Al_2O_3 complex refractive index are of the same order in the mid-infrared range. Thus, if the radiation wavelength $\lambda>10$ μm, the contributions of the absorption and scattering to the radiation attenuation are comparable values.

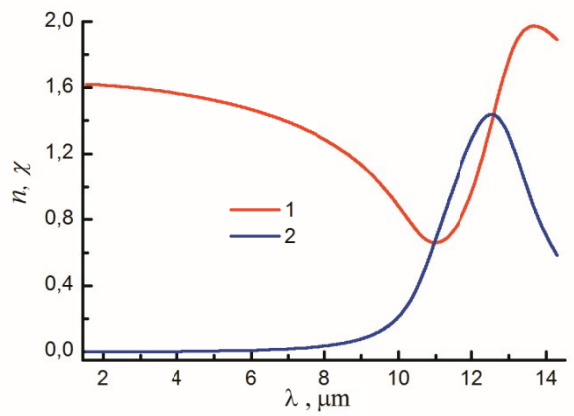

Fig.1. The wavelength dependences of the Al_2O_3 complex refractive index: 1 – $n=n(\lambda)$; 2 – $\chi=\chi(\lambda)$ [4]

Figures 2 to 5 illustrate the calculated dependences of transmission function on the wavelength. The wavelength dependence T(λ) is determined by the spectral features of $\tilde{n}(\lambda)$ and the particle sizes. There is a prominent maximum of each transmission function T(λ) in the considered wavelength range: from 1.54 μm to 14.3 μm. Note that the location of maximums is close to location of the refractive index minimum. The larger an average size of an ensemble of particles, the narrower the wavelength interval at the localization of maximum of the transmission function. For R=10 μm, the transmission function maximum is located within the 8–12 μm wavelength range (see curves 3 and 4 on Figures 3 and 5). For R=2 μm, the maximum is located within the 4–12 μm wavelength range (see curve 2 on Figures 2 and 4). Also this feature can be observed by comparing the curve 1 on Figures 2 and 4. These curves were obtained for the same R=1 μm but for different values of h: 1 m and 10 m. The peak height is 0.1 for h=1 m, and about 0.7 for h=10 m. The curves 1 and 2 (see Figures 3 and 5) was calculated with R=5 μm, and C = $4\cdot10^5$ l^{-1} (curve 1), and C = $2\cdot10^6$ l^{-1} (curve 2). The comparison of these curves shows that the transmission function values change within the [0.88, 0.97] range for lower concentration (see curve 1 on Figures 3 and 5). At the same time, for higher concentration, the change range of T(λ) is 5 times wider (see curve 2 on Figures 3 and 5). The maximum value of the function T(λ) depends on the particles concentration and the optical length. If the path length is fixed, the behavior of the transmission function T(λ) (in particular, a location of the function maximum) depends on the volume concentration of particles. The average particle size uniquely determines the oscillation frequency of T(λ) and the wavelength range in which the maximum of transmission function is localized.

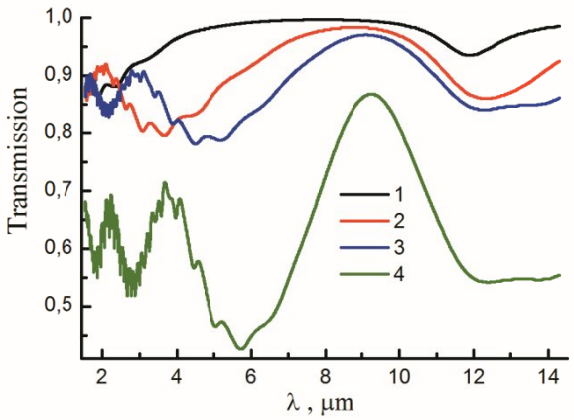

Fig. 2. The wavelength dependence of the transmission function T(λ) for h=1 m, $\tilde{n}=\tilde{n}(\lambda)$ [4]: 1 − R=1 μm, C=10^7 l^{-1}; 2 − R=2 μm, C=$4\cdot10^6$ l^{-1}; 3 − R=3 μm, C =$2\cdot10^6$ l^{-1}; 4 − R=4 μm, C =$4\cdot10^6$ l^{-1}.

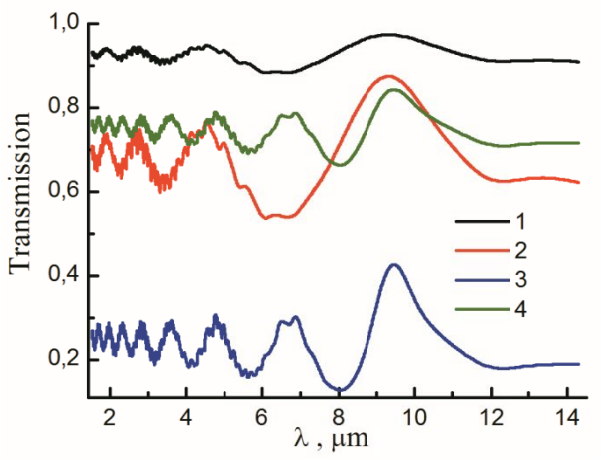

Fig. 3. The wavelength dependence of the transmission function T(λ) for h=1 m, $\tilde{n} = \tilde{n}(\lambda)$ [4]: 1 − R=5 μm, C =4·10^5 l^{-1}; 2 − R=5 μm, C=2·10^6 l^{-1}; 3 − R=10 μm, C =2·10^6 l^{-1}; 4 − R=10 μm, C =4·10^5 l^{-1}.

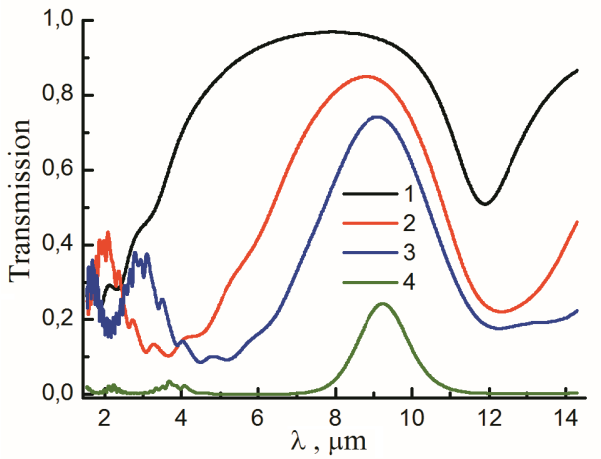

Fig. 4. The wavelength dependence of the transmission function T(λ) for h=10 m, $\tilde{n} = \tilde{n}(\lambda)$ [4]: 1 − R=1 μm, C=10^7 l^{-1}; 2 − R=2 μm, C=4·10^6 l^{-1}; 3 − R=3 μm, C =2·10^6 l^{-1}; 4 − R=4 μm, C =4·10^6 l^{-1}.

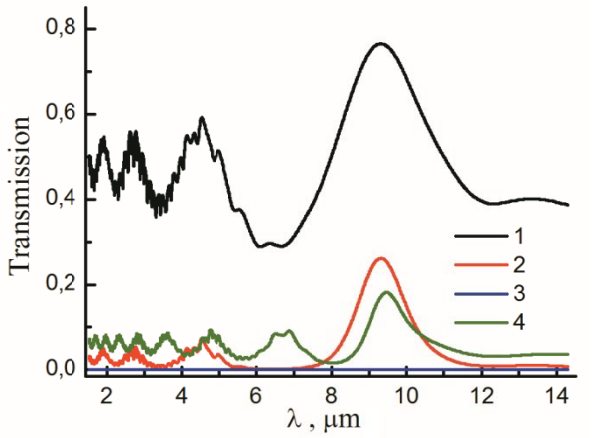

Fig. 5. The wavelength dependence of the transmission function T(λ) for h=10 m, $\tilde{n} = \tilde{n}(\lambda)$ [4]: 1 − R=5 μm, C =4·10^5 l^{-1}; 2 − R=5 μm, C =2·10^6 l^{-1}; 3 − R=10 μm, C =2·10^6 l^{-1}; 4 − R=10 μm, C =4·10^5 l^{-1}.

Figures 6 and 7 illustrate the wavelength dependencies of the extinction, absorption and scattering coefficients for various concentrations and average sizes of particles. These optical characteristics are linearly proportional to the particle concentration (see Eq. (1)). The refraction index and sizes of particles determine the wavenumber dependence of these characteristics. The scattering is the dominant contribution to the radiation extinction for $\lambda < 8$ μm. This is typical for all considered particle sizes. At the same time, the behavior of $n(\lambda)$ determines the features of the wavelength dependence of the scattering coefficient. The oscillations of the scattering coefficient $\alpha_{sca}(\lambda)$ take place when the radiation absorption is negligible and $R \approx \lambda$.

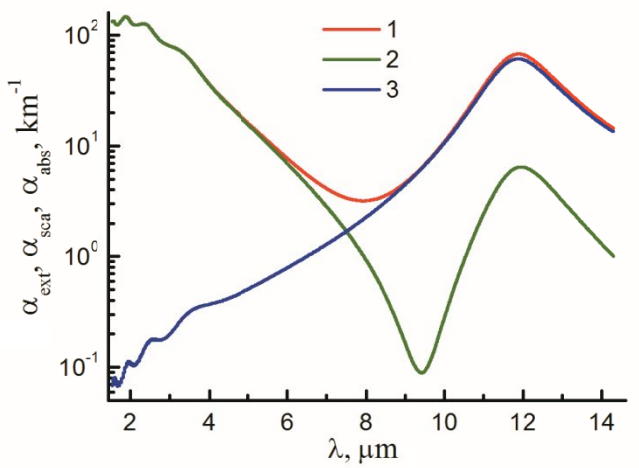

Fig. 6. The wavelength dependence of optical characteristics for R=1 μm, C=10^7 l^{-1}, $\tilde{n} = \tilde{n}(\lambda)$ [4]: 1− extinction coefficient $\alpha_{ext}(\lambda)$; 2− scattering coefficient $\alpha_{sca}(\lambda)$; 3− absorption coefficient $\alpha_{abs}(\lambda)$.

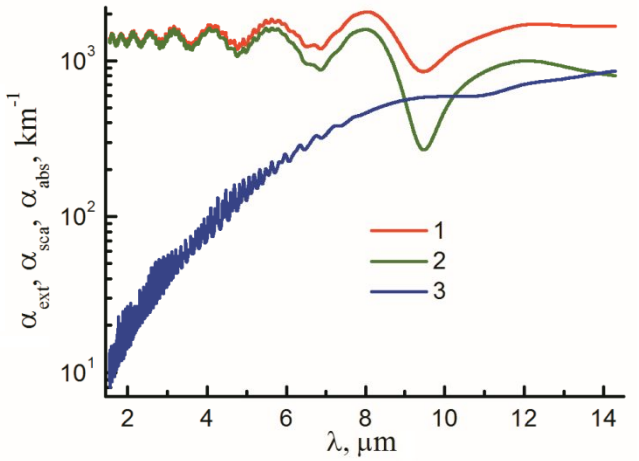

Fig. 7. The wavelength dependence of optical characteristics for R=10 μm, C=$2 \cdot 10^6$ l^{-1}, $\tilde{n} = \tilde{n}(\lambda)$ [4]: 1− extinction coefficient $\alpha_{ext}(\lambda)$; 2− scattering coefficient $\alpha_{sca}(\lambda)$; 3− absorption coefficient $\alpha_{abs}(\lambda)$.

For $\lambda > 8$ μm, the radiation absorption is the dominant contribution to the radiation extinction. However, for $\lambda > 10$ μm and for large particles (R>5 μm), the scattering becomes dominant again. The minimum value of the extinction coefficient $\alpha_{ext}(\lambda)$ is observed at a drastic decrease of the scattering coefficient and the increase of the absorption. Note that for larger particles, the minimum position is shifted to the right. In this spectral range, the extinction coefficient has the minimum value at a maximum value of the absorption coefficient (at λ=12.63 μm n=1.48 χ=1.43). Despite the

absorption index χ has high values at λ>10 μm, the wavelength dependence of the extinction coefficient remains prominent due to the scattering.

CONCLUSION

These studies provide the most promising spectral ranges to get the Al_2O_3 concentration at sensing of jet engine exhaust by quasi monochromatic radiation. The maximum extinction of the radiation by aluminum trioxide takes place in the mid-infrared range. In this spectral range, also it is necessary to take into account the molecular absorption [5–7]. At present, the accuracy of the estimation of extinction by molecular components is significantly improved since the algorithm for calculation of the molecular environments transparency was enhanced and also the known databases on parameters of spectral absorption lines of various gases (including the high temperature databases up to 1000 K) were enhanced [8, 9].

ACKNOWLEDGMENTS

This study was conducted with support of the Ministry of Education and Science of the Russian Federation (project no. 645, project code 4.1349.2014) and with the support from Russian Foundation for Basic Research, grant numbers 13-07-98027 and 15-01-03176.

REFERENCES

[1] Moshkin, K.B., "Calculations and spectrometric measurements of the metal atoms concentration in the liquid rocket engine exhaust for diagnostics of the liquid rocket engines," abstract of a thesis, “Keldyush scientific center”, Moscow (in Russian), 21 p. (2004).

[2] Bohren, C.F., Huffman, D.R., [Absorption and scattering of light by small particles], Wiley, New York, 530 p. (1983).

[3] Zavelevich, F.S., Ushakov, N.N., “Interaction of exhaust jets of rocker propulsions on various propellants with atmosphere for estimation of ecological safety of firing of rockets and launchers,” Vestnik Samarskogo gosudarstvennogo aerokosmicheskogo universiteta (in Russian) 34 (3), 226–234 (2012).

[4] Kischkat, J., Peters, S., Gruska, B., and et. al.,”Mid-infrared optical properties of thin films of aluminum oxide, titanium dioxide, silicon dioxide, aluminum nitride, and silicon nitride,” Appl. Opt. 51, 6789–6798 (2012).

[5] Voitsekhovskaya, O.K., Shefer, O.V., Kashirskii, D.E., “Criterion of the need to consider the cooperative effect of the molecular absorption and aerosol scattering on calculations of IR transmission function,” Proc. SPIE 9292, 92923M-1–92923M-8 (2014).

[6] Voitsekhovskaya, O.K., Voitsekhovskii, A.V., Egorov, O.V., Kashirskii, D.E., “Optical-physical methods of remote diagnostics of high-temperature gas media,” Proc. SPIE 9292, 929211-1–929211-8 (2014).

[7] Voitsekhovskaya, O.K., Egorov, O.V., “Calculation of the intensities of vibrational hydrogen sulfide transitions for remote sounding high-temperature media,” Russian Physics Journal 55(4), 362–368 (2012).

[8] Rothman, L.S., Gordon, I.E., Babikov, Y., and et. al., “The HITRAN–2012 molecular spectroscopic database,” J. Quant. Spectr. Rad. Trans. 130, 4–50 (2013).

[9] Rothman, L.S., Gordon, I.E., Barber, R.J., and et. al., “HITEMP, the high-temperature molecular spectroscopic database,” J. Quant. Spectr. Rad. Trans. 111, 2139–2150 (2010).